Supporting Information

Description of the simulations that quantify effects of chemical exchange

Simulations have been performed that consider an isolated two-site exchanging ^{1}H-^{15}N spin system in order to evaluate the effects of chemical exchange on $R_{\Sigma,\rho} = 1/2(R_{SQ}-R_{MQ,ZO})$, with R_{SQ} and $R_{MQ,ZO}$ defined in the text. The spin system is described in a 31-dimensional vector operator space, which is spanned by the set of operators (in this order): E/2, $\{\mathrm{H}^{\mathrm{A}}_{\mu},\mathrm{N}^{\mathrm{A}}_{\nu},2\mathrm{H}^{\mathrm{A}}_{\mu}\mathrm{N}^{\mathrm{A}}_{\nu}\}_{\mu,\nu\in\{x,y,z\}}$, and $\{\mathrm{H}^{\mathrm{B}}_{\mu},\mathrm{N}^{\mathrm{B}}_{\nu},2\mathrm{H}^{\mathrm{B}}_{\mu}\mathrm{N}^{\mathrm{B}}_{\nu}\}_{\mu,\nu\in\{x,y,z\}}$ where the superscripts *A* and *B* distinguish the two exchanging states,

$$A \underset{k_{\mathrm{BA}}}{\overset{k_{\mathrm{AB}}}{\rightleftarrows}} B. \tag{S1}$$

The time evolution of a vector, **v**, in the vector space spanned by the operators above is described by the solution of the homogeneous master equation

$$\frac{\mathrm{d}}{\mathrm{dt}}\mathbf{v} = -(\mathbf{P}+\mathbf{K})\mathbf{v} \tag{S2}$$

that was given previously in matrix-form[1] in the limit where chemical exchange is neglected. Chemical exchange, as described by eq. S1, is introduced into the computation by an evolution matrix **K**, where,

$$\mathbf{K} = \left(\begin{array}{c|ccc} 0 & 0 & \cdots & 0 \\ \hline 0 & & & \\ \vdots & & \tilde{\mathbf{K}} & \\ 0 & & & \end{array}\right) \tag{S3}$$

and

$$\tilde{\mathbf{K}} = \begin{pmatrix} k_{\mathrm{AB}} & -k_{\mathrm{BA}} \\ -k_{\mathrm{AB}} & k_{\mathrm{BA}} \end{pmatrix} \otimes \mathbf{1}_{15} \tag{S4}$$

with $\mathbf{1}_{15}$ the 15-dimensional identity matrix. The zeros in the first column and first row indicate that the identity operator is unaffected by chemical exchange.

The pulse schemes of Figure 1 are taken into account in each simulation, with pulsed field gradients implemented as pure z-rotations by adding an extra term, $\gamma_{\mathrm{i}}\Delta B(z)$, to the chemical shift of the spins. An average of 120 simulations with linearly spaced $\Delta B(z) \in [-G;G]$ was then performed to approximate the effects of the gradient. At the start of each sequence it is assumed that the initial state corresponds to the one at equilibrium so that $\mathbf{v}_{\mathrm{eq}} = \gamma_{\mathrm{H}}(p_{\mathrm{A}}\mathrm{H}_z^{\mathrm{A}} + p_{\mathrm{B}}\mathrm{H}_z^{\mathrm{B}})$, where $p_{\mathrm{A}} = k_{\mathrm{BA}}/k_{\mathrm{ex}}$ and $p_{\mathrm{B}} = k_{\mathrm{AB}}/k_{\mathrm{ex}}$ are the equilibrium populations of the *A* and *B* conformers, respectively, and $k_{\mathrm{ex}}=k_{\mathrm{AB}}+k_{\mathrm{BA}}$. At the completion of the pulse scheme the state of interest, from which the decay curves $A_{\mathrm{SQ}}(T_{\mathrm{relax}})$, $A_{\mathrm{MQ,ZO}}(T_{\mathrm{relax}})$ and $\beta = A_{\mathrm{SQ}}(T_{\mathrm{relax}})/A_{\mathrm{MQ,ZO}}(T_{\mathrm{relax}})$ are generated, depends on the exchange rate. Thus, for $k_{\mathrm{ex}} < \sqrt{\Delta\omega_{\mathrm{H}}^2 + \Delta\omega_{\mathrm{N}}^2}$ slow exchange has been assumed and the magnetization from state *A* has been used to generate each of the decay curves, while for $k_{\mathrm{ex}} > \sqrt{\Delta\omega_{\mathrm{H}}^2 + \Delta\omega_{\mathrm{N}}^2}$ the sum of magnetization from states *A* and *B* (fast exchange limit) has been retained to calculate the curves. Once the value of β is calculated $R_{\Sigma,\rho}$ is generated via a least-squares fit of an exponential function, $A\exp(-2R_{\Sigma,\rho}T_{\mathrm{relax}})$, to the decay of β vs T_{relax}. Finally, R_{dd} is obtained from eq. 11.2 of the text where $\sin\theta_{\mathrm{H}}$ and $\sin\theta_{\mathrm{N}}$ are calculated from the position of the major peak (*i.e.*, the peak with chemical shift closest to ω^{A}, the offset of the major species, see below), as determined from the eigenvalues of the two-site exchange matrix.

As described in detail in the text four experiments are recorded that encode the decay rates, $R_{1\rho}(2H'_zN_z)$, $R_{1\rho}(2H_zN'_z)$, $R_{1\rho^2}(2H'_zN'_z)$ and $R_1(2H_zN_z)$ and the desired experimental rate, $R_{SQ} - R_{MQ,ZO}$ is obtained from fits of the ratio $A_{SQ}(T_{relax})/A_{MQ,ZO}(T_{relax})$. In the simulations exactly the same procedure is employed. The field strength of spin-lock pulses and the length of delays are as given in the legend to Figure 2. In addition, $\omega_H^A/2\pi = -100$ Hz, $\omega_H^B/2\pi = 450$ Hz, $\omega_N^A/2\pi = -100$ Hz, $\omega_N^B/2\pi = 500$ Hz, λ_H = 1s^{-1}, $\vartheta_H = 10$ s^{-1}, $\Delta\sigma_N = -172$ ppm, $\Delta\sigma_H\sqrt{(1+\eta_H^2/3)/3} =$ 10 ppm, J_{HN}= −92 Hz, r_{HN} = 1.02 Å, and B_0 = 14.1 T, where $\omega_H^A(\omega_N^A)$ and $\omega_H^B(\omega_N^B)$ are the proton (nitrogen) Larmor frequencies for the two chemically exchanging conformations *A* and *B*, respectively, and the other parameters are defined in the text. The power spectral density function of the ^{1}H–^{15}N vector was described by a simple Lipari-Szabo[2,3] model,

$$J(\omega) = \frac{2}{5}\left(\frac{S^2\tau_M}{1+\omega^2\tau_M^2} + \frac{\left(1-S^2\right)\tau_e}{1+\omega^2\tau_e^2}\right) \tag{S5}$$

with an order parameter S^2 = 0.80, a correlation time for overall molecular tumbling τ_M=10 ns, and a correlation time for the fast internal motion, $\tau_i^{-1} = \tau_e^{-1} - \tau_M^{-1} = 0.1$ ns. Values of the rate constant, k_{ex}, and the population of the exited state, p_B, eq. S1, were varied from 10 s^{-1} to 10^6 s^{-1} and from 0 to 10%, respectively. Figure 2 establishes that chemical exchange introduces a systematic error of less than 1% in the obtained R_{dd} rate.

J(0) extracted from the R_{dd} rate by reduced spectral density mapping is essentially independent of the CSA tensor

As described in the text and illustrated in Figure 2 and eq. 6 of the text the R_{dd} rate depends solely on dipole-dipole interactions and is independent of the magnitude of the ^{15}N CSA tensor, $\Delta\sigma_N$. However, R_{dd} is given by a linear combination of spectral densities evaluated at $\omega = 0$, ω_N and $0.87\omega_H$, and hence $J(\omega_N)$, $J(0.87\omega_H)$ must be known *a priori* in order to extract $J(0)$, eq. 13. The values of $J(\omega_N)$ and $J(0.87\omega_H)$ can be obtained from the ^{15}N R_1 rate and the ^{1}H-^{15}N NOE, but their values will depend on the choice of $\Delta\sigma_N$ because R_1 and NOE are a function of $\Delta\sigma_N$. Fortunately, the contribution of $J(\omega_N)$ and $J(0.87\omega_H)$ to R_{dd} is minor in the macromolecular limit so that it is expected that $J(0)$ will be insensitive to the choice of $\Delta\sigma_N$. Figure S1 demonstrates that this is the case, with errors in extracted $J(0)$ values of less than 1% for $\Delta\sigma_N$ that deviates by 10 ppm from the assumed value. In contrast, significantly larger errors are introduced into $J(0)$ obtained from a reduced spectral density mapping of the form $\{R_2(N_x), R_1(N_z), {}^1\text{H-}^{15}\text{N NOE}\} \mapsto \{J(0), J(\omega_N), J(0.87\omega_H)\}$.

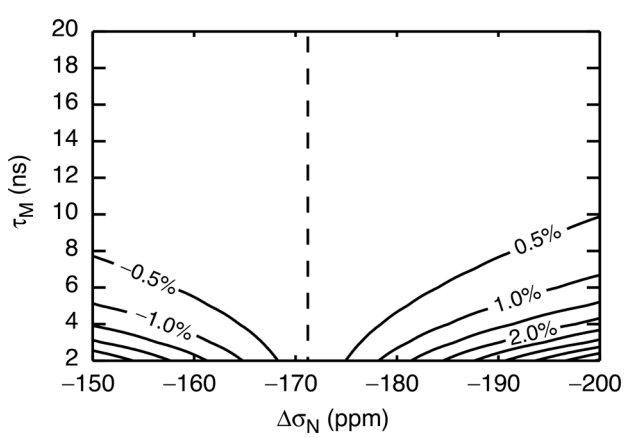

Figure S1. Contour plots of the relative deviation, $(J(0)_{Rdd}-J(0))/J(0)$ as a function of overall rotational correlation times, τ_M, and CSA tensor values, $\Delta\sigma_N$. R_{dd}, $R_1(N_z)$ and ^{1}H-^{15}N NOE rates were simulated using

Eq. S5, with S^2=0.8, τ_e=100 ps and a static magnetic field strength of B_0=14.1 T; subsequently, $J(0)_{Rdd}$ was obtained by reduced spectral density function mapping, $\{R_{dd}, R_1(N_z), {}^1H\text{-}{}^{15}N$ NOE$\} \mapsto \{J(0)_{Rdd}, J(\omega_N), J(0.87\omega_H)\}$, assuming $\Delta\sigma_N$= −172 ppm.

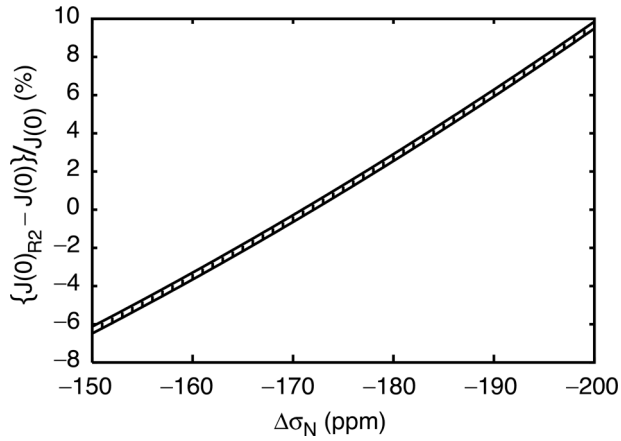

Figure S2. $(J(0)_{R2}-J(0))/J(0)$ derived for different CSA tensor values, $\Delta\sigma_N$. The vertical lines indicate the range obtained by varying the overall rotational correlation time τ_M from 2 ns to 20 ns. Values of $J(0)_{R2}$ were obtained from the mapping $\{R_2(N_x), R_1(N_z), {}^1H\text{-}{}^{15}N$ NOE$\} \mapsto \{J(0)_{R2}, J(\omega_N), J(0.87\omega_H)\}$, with relaxation parameters and spectral densities, $J(\omega)$, calculated using the same parameters listed in the legend to Figure S1.

References

(1) Allard, P.; Helgstrand, M.; Hard, T., *J. Magn. Reson.* **1998**, *134*, 7-16.
(2) Lipari, G.; Szabo, A., *J. Am. Chem. Soc.* **1982**, *104*, 4559-4570.
(3) Lipari, G.; Szabo, A., *J. Am. Chem. Soc.* **1982**, *104*, 4546-4559.